JACS
JOURNAL OF THE AMERICAN CHEMICAL SOCIETY
Article
pubs.acs.org/JACS

Synthesis and N−H Reductive Elimination Study of Dinuclear Ruthenium Imido Dihydride Complexes

Shin Takemoto,* Yusuke Yamazaki, Takahiro Yamano, Daichi Mashima, and Hiroyuki Matsuzaka*

Department of Chemistry, Graduate School of Science, Osaka Prefecture University, Gakuen-cho 1-1, Naka-ku, Sakai, Osaka 599-8531, Japan

Supporting Information

ABSTRACT: Diruthenium imido dihydride complexes $[(Cp^*Ru)_2(\mu\text{-NAr})(\mu\text{-H})_2]$ (Ar = Ph (**2a**), *p*-$MeOC_6H_4$ (**2b**), *p*-ClC_6H_4 (**2c**), 2,6-$Me_2C_6H_3$ (**2d**); Cp^* = η^5-C_5Me_5) have been synthesized by hydrogenation of the corresponding bis(amido) complexes $[Cp^*Ru(\mu\text{-NHAr})]_2$ (**1a−d**). Reductive elimination of the N−H bond from **2a−c** in the presence of arene yields the amido hydride complexes $[(Cp^*Ru)_2(\mu\text{-NHAr})(\mu\text{-H})(\mu\text{-}\eta^2\text{:}\eta^2\text{-arene})]$ containing a π-bound arene. The rate and kinetic isotope effect for this reaction are consistent with a mechanism involving initial rate-determining reductive elimination of an N−H bond to produce the coordinatively unsaturated amido hydride species $\{(Cp^*Ru)_2(\mu\text{-NHAr})(\mu\text{-H})\}$ (**A**) followed by rapid trapping of this species by an arene. The existence of **A** is also supported by the reversible interconversion of $[(Cp^*Ru)_2(\mu\text{-NHPh})(\mu\text{-H})(\mu\text{-}\eta^2\text{:}\eta^2\text{-}C_7H_8)]$ with the tetranuclear complex $[(Cp^*Ru)_4(\mu_4\text{-NHPh})(\mu\text{-NHPh})(\mu\text{-H})_2]$ (**4**), a dimerization product of **A** through a μ_4-NHPh bridge. DFT calculations provide structures of **A** and transition states for the N−H reductive elimination. Two distinct reaction pathways are found for the N−H reductive elimination, one of which involves direct migration of a μ-hydride to the μ-NAr ligand, and the other involves formation of a transient terminal hydride species.

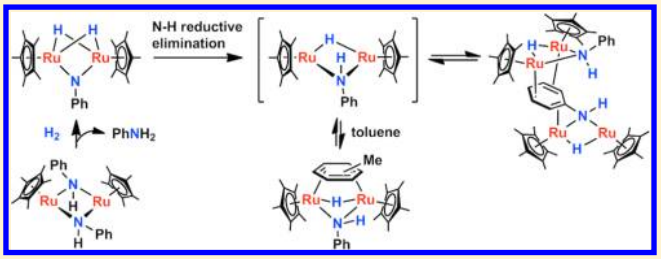

INTRODUCTION

Reductive elimination of a N−H bond is a fundamental organometallic process of considerable importance in understanding metal-mediated N−H bond-forming and -breaking processes. One of such processes of great interest is the stepwise N + H addition reaction in the catalytic synthesis of ammonia over solid-state iron and ruthenium catalysts.[1] Although recent computational studies have provided a detailed picture of this N−H bond-forming process,[2] potentially useful information will be obtained from the study of relevant N−H bond-forming reactions in homogeneous transition metal complexes.

Studies on the reductive elimination of N−H bond have mainly concerned amido hydride complexes of late transition metals.[3] Trogler reported the reductive elimination of aniline from *trans*-$[PtH(NHPh)(PEt_3)_2]$, which was proposed to be associatively induced by added substrates such as PEt_3, CO, and H_2.[3a] Bergman studied the kinetics of PPh_3-induced reductive elimination of RNH_2 from $[Cp^*Ir(NHR)H(PPh_3)]$ and proposed a mechanism involving initial rearrangement of η^5-Cp^* to η^3-Cp^* followed by coordination of PPh_3 and elimination of RNH_2.[3b] Hartwig and Goldman recently reported a direct spontaneous reductive elimination of N−H bond from $[(PCP)Ir(NH_2)H]$ to give $[(PCP)Ir(NH_3)]$,[3c] and Brookhart reported a similar chemistry in arylamido complexes of the type $[(POCOP)Ir(NHAr)H]$.[3d]

Transition metal imido complexes have attracted attention as models for surface-bound metal imides and nitrides.[4] Heterolytic addition of H_2 to metal−nitrogen multiple bonds of imido complexes[5] as well as nitride[6,7] and dinitrogen[8] complexes of imido-like bonding has been well documented. In contrast, only a small number of imido hydride complexes have been shown to undergo N−H reductive elimination when treated with external substrates such as CO,[9] PMe_3,[10] and H_2.[11] In none of these cases has the mechanism of the N−H bond-forming step been studied in considerable detail.

Ruthenium is one of the best elemental catalysts for N_2 reduction,[12] and several polynuclear ruthenium complexes related to metal-mediated N−H bond-forming and -breaking processes have been reported. Suzuki et al. studied a series of triruthenium μ_3-imido hydride clusters of the type $[(Cp^*Ru)_3(\mu_3\text{-NR})(\mu\text{-H})_3]$ in their work on the activation of ammonia, hydrazines, and azobenzene by $[(Cp^*Ru)_3(\mu\text{-H})_3(\mu_3\text{-H})_2]$.[13] Diruthenium amido hydride complexes have been prepared by reduction of organonitriles,[14] hydrazine,[15] or azide[16] on diruthenium complexes. To our knowledge, diruthenium imido hydride complexes have not been reported, although a local $Ru_2(\mu\text{-NH})(\mu\text{-H})$ structure has been proposed in a transition state of NH + H addition reaction on a ruthenium surface.[2a,b]

We have recently developed a synthetic method for dinuclear ruthenium imido complexes of the type $[(Cp^*Ru)_2(\mu\text{-NPh})(\mu\text{-L})]$ (L = CO, CH_2, and related ligands).[17] We now report synthesis of imido dihydride complexes of the type $[(Cp^*Ru)_2(\mu\text{-NAr})(\mu\text{-H})_2]$. This article describes the synthesis

Received: January 18, 2012
Published: September 13, 2012

dx.doi.org/10.1021/ja3005682 | J. Am. Chem. Soc. 2012, 134, 17027−17035

and characterization of these dinuclear imido dihydride complexes and the study of their N−H reductive coupling reactivity, including characterization of amido hydride derivatives and kinetic and computational studies of the N−H bond-forming step.

RESULTS AND DISCUSSION

Synthesis of Imido Dihydride Complexes. Treatment of $[Cp^*Ru(\mu\text{-}NHPh)]_2$ (**1a**)[18] with 1 atm of H_2 at −80 °C in toluene followed by warming to room temperature with stirring over 2 h afforded the imido dihydride complex $[(Cp^*Ru)_2(\mu\text{-}NPh)(\mu\text{-}H)_2]$ (**2a**) in 71% yield as monitored by ^{1}H NMR spectroscopy (eq 1).[19] Prolonged reaction of **2a** with H_2 (12 h)

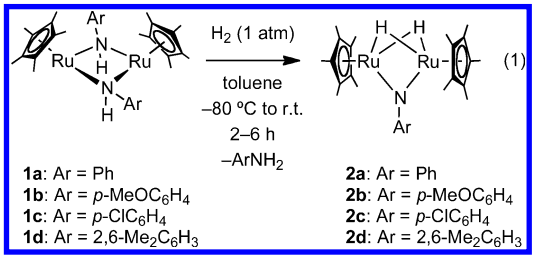

resulted in hydrogenolysis of **2a** to $[(Cp^*Ru)_2(\mu\text{-}H)_4]$[20] and aniline. Since **2a** underwent N−H reductive elimination even at room temperature to give the amide hydride toluene complex $[(Cp^*Ru)_2(\mu\text{-}NHPh)(\mu\text{-}H)(\mu\text{-}\eta^2\text{:}\eta^2\text{-}C_7H_8)]$ (**3a**; vide infra), **2a** was characterized spectroscopically without isolation. Substituted arylamido complexes $[Cp^*Ru(\mu\text{-}NHAr)]_2$ (Ar = *p*-$MeOC_6H_4$ (**1b**), *p*-ClC_6H_4 (**1c**), 2,6-$Me_2C_6H_3$ (**1d**)) also reacted with H_2 to give the corresponding imido dihydride complexes **2b**−**d** (eq 1), which were thermally more robust than **2a** and could be isolated as analytically pure red crystalline solids in 61%, 67%, and 74% yield, respectively.

The ^{1}H NMR spectrum of **2a** in C_6D_6 showed the hydride resonance at δ −11.25 in 2H intensity relative to the 30H signal of C_5Me_5 at δ 1.83. Variable-temperature T_1 measurement gave the T_1 minimum of 468 ms (500 MHz, −80 °C) for the hydride resonance, a value consistent with a classical dihydride formulation.[21] The IR spectrum of **2a** (Nujol) showed a weak band at 1643 cm^{-1} assignable to a ν(Ru−H) stretch for the bridging hydride ligands.[22] **2b**−**d** also showed similar spectroscopic features except that the ν(Ru−H) band for **2d** was too weak to be assigned unambiguously. The assignment of ν(Ru−H) bands in **2a**−**c** was confirmed by the disappearance of these bands in the IR spectra of corresponding d_2 isotopomers $[(Cp^*Ru)_2(\mu\text{-}NAr)(\mu\text{-}D)_2]$, although ν(Ru−D) bands in these complexes were obscured by overlapping with other peaks.

To gain insight into the mechanism of the formation of **2a**−**d**, **1a** was treated with D_2 in toluene-d_8. This produced the imido dideuteride complex **2a**-d_2 (87%) and $PhNH_2$ (100%) as monitored by ^{1}H NMR spectroscopy (eq 2). The reaction proceeded similarly in nondeuterated toluene to give **2a**-d_2 and $PhNH_2$. These results suggest that **2a** was formed by initial oxidative addition of H_2 to **1a** followed by elimination of aniline via α-abstraction (i.e., proton transfer from one anilido ligand to the other). This type of addition−elimination sequence has also been proposed for the reaction of **1a** with dative two-electron ligands such as CO.[17a] The α-abstraction from amido complexes is an established route to transition metal imido complexes and has been induced thermally or by addition of dative ligands.[23] To our knowledge, the synthesis of **2a**−**d**,

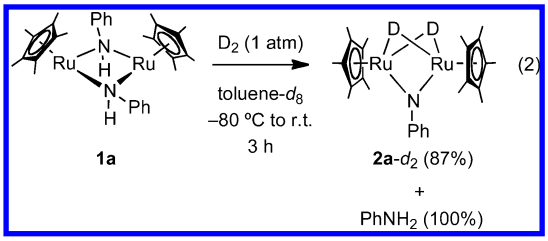

demonstrates for the first time that α-abstraction from amido complexes can be induced by oxidative addition of H_2.

To probe the possibility of H−H bond formation in **2a**−**d**, an H/D exchange reaction was attempted. When a solution of **2a**-d_2 in C_6D_6 was stirred under 1 atm of H_2 at room temperature for 20 h, no reaction took place. This lack of H/D exchange indicates that **2a**-d_2 does not reductively eliminate D_2 under the conditions employed. In contrast, the tetradeuteride complex $[(Cp^*Ru)_2(\mu\text{-}D)_4]$ was reported to undergo an H/D exchange reaction with 1 atm of H_2 at room temperature to give $[(Cp^*Ru)_2(\mu\text{-}H)_4]$ quantitatively.[20]

Formation of Amido Hydride Complexes. The imido dihydride complex **2a** underwent N−H reductive elimination at room temperature in toluene over the course of 12 h to yield the amido hydride toluene complex **3a** quantitatively (eq 3).

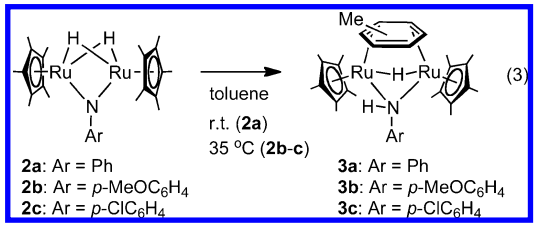

Complexes **2b**,**c** reacted similarly to give the corresponding amido hydride toluene complexes **3b**,**c**. In contrast, **2d** remained intact even after heating at 110 °C in toluene for 12 h. When **2a** was allowed to react in nonaromatic solvent (i.e., cyclohexane or THF), a complicated mixture of products including the tetranuclear amido hydride complex **4** (vide infra) was produced.

Complex **3a** was isolated in 68% yield (based on **1a**) as a red crystalline solid and characterized by analytical and spectroscopic techniques. The ^{1}H NMR spectrum of **3a** in C_6D_6 showed signals assignable to the hydride and N−H protons at δ −13.72 (s, 1H) and −1.38 (br, 1H), respectively, along with a C_5Me_5 signal at δ 1.50 (s, 30H). The signals of the toluene unit were observed as free molecule at 22 °C, indicating that toluene was displaced by C_6D_6. However, at −80 °C in THF-d_8 in the presence of 10 equiv of toluene (added to suppress dissociation of toluene from **3a**), five distinct aryl protons for the μ-η^2:η^2-toluene ligand (δ 5.67 (1H), 3.03 (1H), 2.91 (1H), 2.86−2.79 (2H)) and two inequivalent Cp* groups were observed in the ^{1}H NMR spectrum of **3a**, indicating that dissociation of toluene was very slow at this temperature. The IR spectrum of **3a** showed weak bands at 3210 and 1597 cm^{-1} assignable to ν_{NH} and ν_{RuH}, respectively, the latter being consistent with the bridging hydride formulation.[22,24] To provide additional support for the structure of **3a**, the μ-η^2:η^2-naphthalene analogue $[(Cp^*Ru)_2(\mu\text{-}NHPh)(\mu\text{-}H)(\mu\text{-}\eta^2\text{:}\eta^2\text{-}C_{10}H_8)]$ (**5a**) was prepared by ligand exchange from **3a** and characterized by X-ray analysis (Figure 1). In contrast to **3a**, the signals of the bound naphthalene moiety in **5a** were identified in its ^{1}H and ^{13}C{^{1}H} NMR spectra even at room temperature. The chemical shifts of the μ-hydride,

dx.doi.org/10.1021/ja3005682 | J. Am. Chem. Soc. 2012, 134, 17027−17035

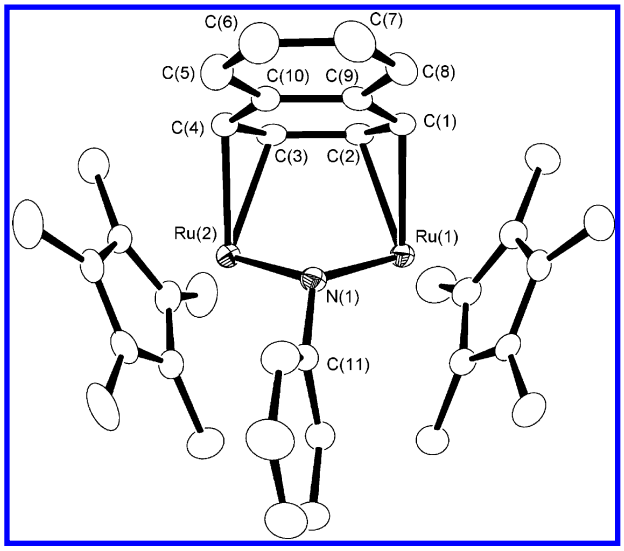

Figure 1. ORTEP drawing of **5a** with 30% ellipsoids. Selected interatomic distances (Å): Ru(1)···Ru(2) = 2.8428(9); Ru(1)−N(1) = 2.119(3); Ru(1)−C(1) = 2.216(4); Ru(1)−C(2) = 2.193(4); Ru(2)−N(1) = 2.130(3); Ru(2)−C(3) = 2.181(4); Ru(2)−C(4) = 2.217(4); N(1)−C(11) = 1.415(5); C(1)−C(2) = 1.420(6); C(2)−C(3) = 1.445(6); C(3)−C(4) = 1.420(6).

N−H, and Cp* protons in **5a** (δ −13.44, −1.26, and 1.50, respectively) were quite similar to those of **3a**, indicating similar solution structures for these compounds.

When **3a** was dissolved in THF, the μ-η^2:η^2-toluene ligand was easily liberated, and the tetranuclear complex **4** was produced quantitatively (eq 4). **4** regenerated **3a** upon dissolution

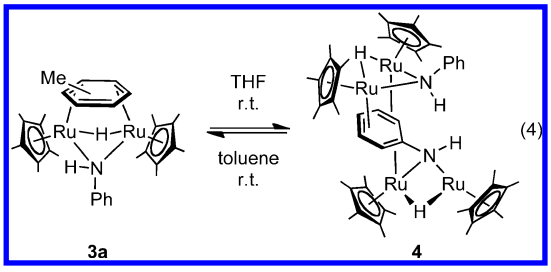

in toluene. **4** was isolated in 79% yield as red block crystals from THF−MeCN and characterized by X-ray diffraction (Figure 2). The tetranuclear structure consists of two {(Cp*Ru)$_2$(μ-NHPh)(μ-H)} units linked through η^2:η^2-coordination of a phenyl group, resulting in an unprecedented μ_4-anilido ligand. The η^2:η^2-arene-bonded diruthenium unit (Ru(3)−Ru(4)) has a structure analogous to that of **5a**, while the other diruthenium unit (Ru(1)−Ru(2)) has no additional arene and contains a μ-κ^1:η^3-NHPh ligand. This type of μ-κ^1:η^3-enamide structure is uncommon. The closest precedent is the aza-π-allyl ligand in [(Cp*Ru)$_2$(μ-H)(μ-NPr^{i}C$_3$H$_5$)].[25]

The ^{1}H NMR spectrum of **4** in THF-d_8 showed four inequivalent Cp* signals at δ 1.78, 1.67, 1.56, and 1.46 in equal intensity, indicating that the dimeric tetranuclear structure was maintained in solution. The π-bound phenyl ring was clearly identified by the characteristic upfield signals at δ 2.73 (3H), 2.50 (1H), and 1.96 (1H). The N−H resonances were found at δ 0.66 and 5.10, the latter downfield signal being likely due to the μ_4-NHPh moiety. Two hydride resonances were observed at δ −9.49 and −13.63.

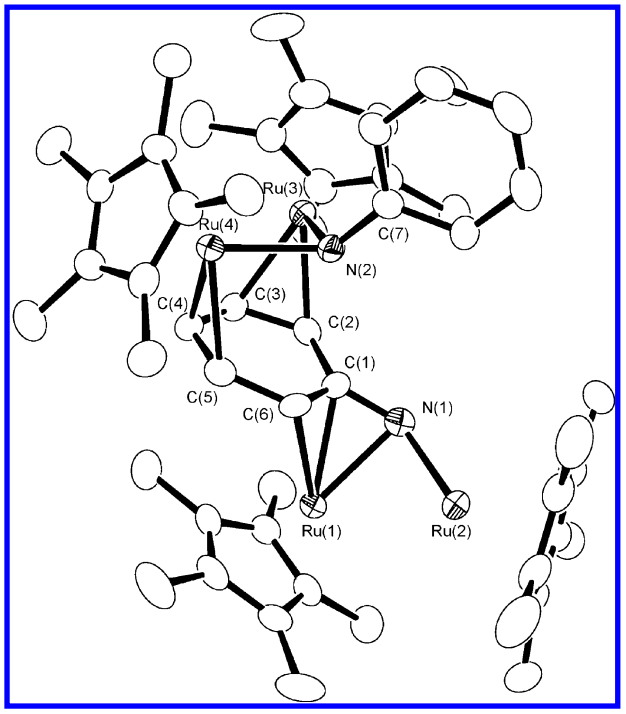

Figure 2. ORTEP drawing of **4** with 30% ellipsoids. Selected interatomic distances (Å): Ru(1)···Ru(2) = 2.7304(14); Ru(1)−N(1) = 2.177(10); Ru(1)−C(1) = 2.229(11); Ru(1)−C(6) = 2.239(11); Ru(2)−N(1) = 2.082(10); Ru(3)···Ru(4) = 2.8638(16); Ru(3)−N(2) = 2.128(9); Ru(3)−C(2) = 2.225(12); Ru(3)−C(3) = 2.155(11); Ru(4)−N(2) = 2.108(8); Ru(4)−C(4) = 2.180(12); Ru(4)−C(5) = 2.246(12); N(1)−C(1) = 1.356(14); N(2)−C(7) = 1.399(13); C(1)−C(2) = 1.440(15); C(2)−C(3) = 1.408(15); C(3)−C(4) = 1.441(16); C(4)−C(5) = 1.442(15); C(5)−C(6) = 1.436(16); C(1)−C(6) = 1.388(17).

Although **2d** did not undergo N−H reductive elimination under thermal conditions in toluene at 110 °C (vide supra), it smoothly reacted with carbon monoxide at room temperature to give the N−H bond-formed product **6** having two terminal CO ligands (eq 5). **6** was isolated in 70% yield as a red crystalline solid and characterized by standard analytical and spectroscopic techniques.

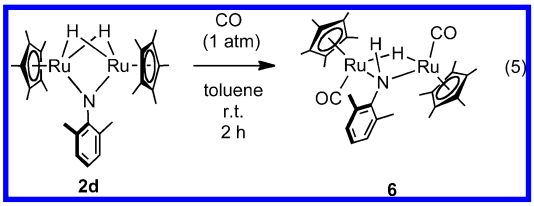

Kinetic Study of N−H Reductive Elimination. To investigate the mechanism of N−H reductive elimination in **2a−c**, a kinetic study was examined. We devised a reaction shown in eq 6, in which the isolable imido dihydride complex **2b** was treated with excess C$_6$D$_6$ in cyclohexane-d_{12} to give the amido hydride μ-η^2:η^2-C$_6$D$_6$ complex **3b′** (the same species formed when **3b** was dissolved in C$_6$D$_6$). The progress of the reaction was followed by ^{1}H NMR spectroscopy, and the observed rate constants are summarized in Table 1.

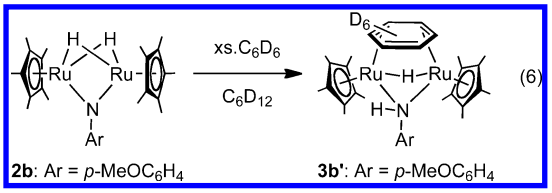

dx.doi.org/10.1021/ja3005682 | J. Am. Chem. Soc. 2012, 134, 17027−17035

Table 1. Rate Constants for the Reaction of 2b with Excess L in Cyclohexane-d_{12}

$[\mathbf{2b}]_0$ (mol L^{-1})	L	[L] (mol L^{-1})	T (°C)	k_{obs} (s^{-1})
0.059	C_6D_6	1.2	25	2.2×10^{-5}
0.059	C_6D_6	1.2	30	4.0×10^{-5}
0.060	C_6D_6	1.2	35	6.5×10^{-5}
0.059	C_6D_6	1.2	40	1.3×10^{-4}
0.059	C_6D_6	1.2	45	2.3×10^{-4}
0.057	C_6D_6	1.7	35	6.0×10^{-5}
0.053	C_6D_6	2.1	35	6.4×10^{-5}
0.052	C_6D_6	2.6	35	5.9×10^{-5}
0.060	$C_{10}H_8$	1.2	35	6.5×10^{-5}

The reaction was found to be cleanly first-order in [**2b**] and showed zero-order dependence on $[C_6D_6]$. Rate measurement at five different temperatures from 25 to 45 °C gave the following activation parameters: E_a = 22(1) kcal mol^{-1}, $\Delta H^{\ddagger}$ = 22(1) kcal mol^{-1}, and $\Delta S^{\ddagger}$ = 6(3) eu (Figure 3).

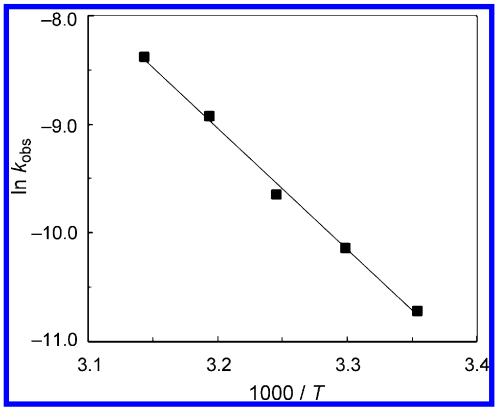

Figure 3. Arrhenius plot for the conversion of **2b** to **3b′** at 25−45 °C.

The rate was also measured for the reaction of **2b** with excess naphthalene in cyclohexane-d_{12} to form [$(Cp^*Ru)_2(\mu$-NHAr)-$(\mu$-H)$(\mu$-η^2:η^2-$C_{10}H_8)$] (**5b**); the observed rate constant for

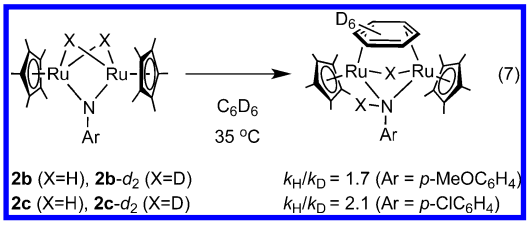

Scheme 1

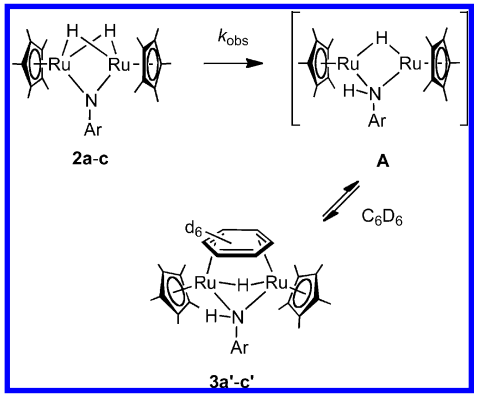

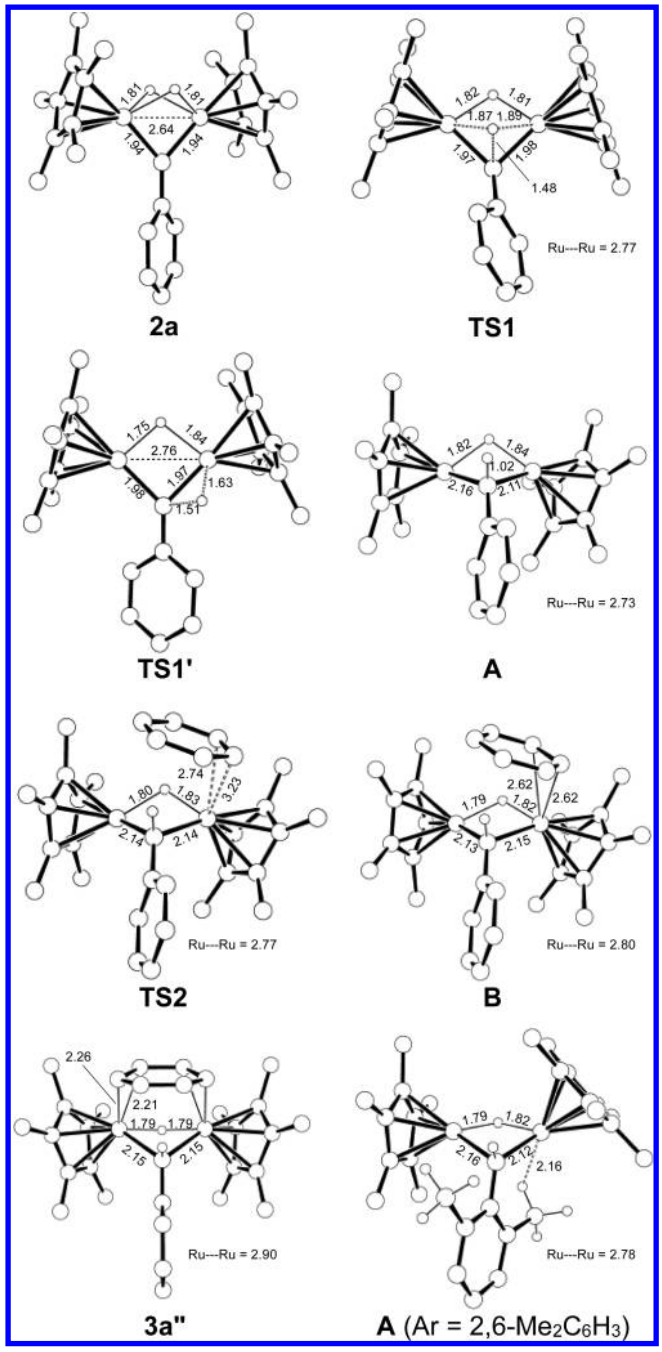

Figure 4. Optimized structures of local minima and transition states in **2a** + C_6H_6 → **3a″** in C_6H_6 (M06, PCM). The optimized structure of **A** (Ar = 2,6-$Me_2C_6H_3$) is also shown. Hydrogen atoms on C_5Me_5 groups and aryl rings are omitted for clarity. Interatomic distances are given in Å.

this reaction (6.5×10^{-5} s^{-1} at 35 °C) was identical to that for the reaction in eq 6 ($6.2(3) \times 10^{-5}$ s^{-1}). These results suggest that the entering arene molecule is not involved in the rate-determining step.

To explore the nature of the rate-determining step, we examined the kinetic isotope effect (KIE) by comparing the rates of reactions of **2b** and **2b**-d_2 in C_6D_6 (eq 7). We observed a normal kinetic isotope effect of k_H/k_D = 1.7 ($k_H = 4.1 \times 10^{-5}$ vs $k_D = 2.4 \times 10^{-5}$ s^{-1}), which indicates that the rate-determining step involves dissociation of a Ru−H bond. We also examined KIE for **2c** and **2c**-d_2 (eq 7) and obtained k_H/k_D = 2.1 ($k_H = 4.0 \times 10^{-5}$ vs $k_D = 1.9 \times 10^{-5}$ s^{-1}). Interestingly, the rates of

dx.doi.org/10.1021/ja3005682 | J. Am. Chem. Soc. 2012, 134, 17027−17035

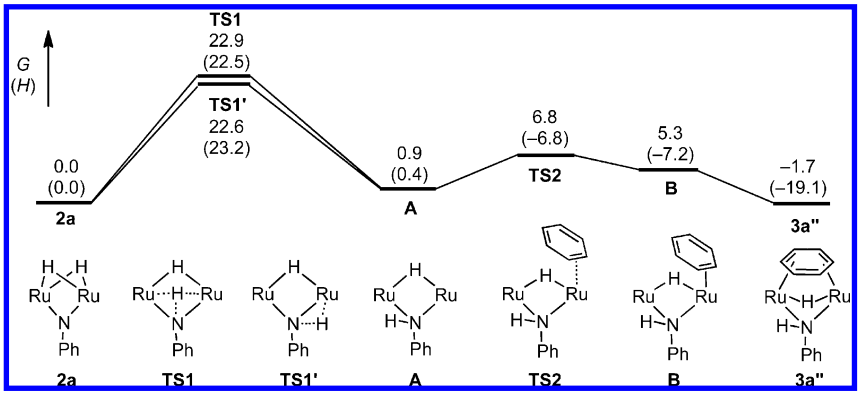

Figure 5. Gibbs free energy profile for **2a** + C_6H_6 → **3a″** in C_6H_6 (M06, PCM). Energies (kcal mol^{-1}) are relative to **2a** + C_6H_6. Enthalpies are given in parentheses.

reactions of **2b** and **2c** (and **2b**-d_2 and **2c**-d_2) are quite similar despite the opposing electronic effect of the *p*-MeO and *p*-Cl substituents. The electron-donating *p*-MeO group would enhance the basicity of the imido nitrogen but might retard the reductive elimination from ruthenium centers, whereas electron-withdrawing *p*-Cl substituent would impart opposite effects. This could be a possible reason for the similar kinetics of the reactions of **2b** and **2c**.

Possible reactivity patterns of **2a**–**c** that involve the Ru–H bond dissociation would include (i) the reductive elimination of an N–H bond, (ii) bridge-to-terminal rearrangement of a hydride ligand, and (iii) reductive H–H coupling to form an η^2-dihydrogen complex. The activation energy for the conversion of a Ru–H–Ru bridge to a terminal Ru–H and an unbridged Ru–Ru bond has been estimated to be 10 kcal mol^{-1}.[26] Thus, the bridge-to-terminal hydride rearrangement is unlikely to dominate the overall rate of the present reaction whose E_a is estimated to be 22 kcal mol^{-1}. The formation of an η^2-dihydrogen complex is also unlikely given the absence of H/D exchange between **2a**-d_2 and H_2 (vide supra). Therefore, the rate-determining dissociation of a Ru–H bond in **2a**–**c** is most likely attributed to the reductive elimination of an N–H bond.

The simplest mechanism consistent with these observations involves initial rate-determining reductive elimination of an N–H bond to form the unsaturated amido hydride intermediate [(Cp*Ru)$_2$(μ-NHAr)(μ-H)] (**A**) followed by rapid trapping of this species by an arene molecule (Scheme 1). The facile interconversion between **3a** and **4** (eq 4) also strongly suggests the existence of the intermediate **A**.

Computational Study. To explore the nature of the unsaturated amido hydride intermediate and the transition state of the N–H bond formation, we performed a computational study based on density functional theory (DFT). Here we mainly discuss the results obtained by calculations at the M06 level, but some data obtained at the B3PW91 level are also used.

We initially examined the reaction of **2a** with benzene to give [(Cp*Ru)$_2$(μ-NHPh)(μ-H)(μ-η^2:η^2-C_6H_6)] (**3a″**). Optimized structures on the potential energy surface of **2a** + C_6H_6 → **3a″** are shown in Figure 4, and a Gibbs free energy profile for this reaction is given in Figure 5.

The optimized structure of **2a** has an approximate C_2 symmetry with the two Cp* groups taking a staggered orientation and the phenyl ring being tilted from the Ru_2N plane (dihedral angle 45.4°). The hydride ligands symmetrically bridge the Ru atoms with Ru–H distances (1.81–1.83 Å) similar to those in [(Cp*Ru)$_2$(μ-H)$_4$].[20,26b] The Ru–N distances (1.94 Å) are typical of μ-imido ligands of Ru–N multiple bond character.[17,27]

As shown in Figure 5, **2a** was found to give the amido hydride complex **A** via the transition state **TS1** or via the transition state **TS1′** with activation energies of 22.9 and 22.6 kcal mol^{-1}, respectively. In **TS1** the migrating hydrogen atom bridges the Ru_2N triangle, whereas in **TS1′** the migrating hydrogen atom bridges one of the Ru–N bonds. These results suggest that the N–H reductive elimination from **2a** may proceed either by maintaining the bridging hydride structure or by the formation of a terminal hydride ligand. This N–H reductive elimination step is rate-determning in the overall reaction. We could not find any stable imido dihydride benzene adduct, which would be formed if the reaction of **2a** and C_6H_6 proceeded via initial coordination of C_6H_6. Attempts to locate such adducts led to collapse to **2a** and free C_6H_6.

The optimized structure of **A** (Figure 4) shows a pyramidal two-legged piano stool geometry at both Ru centers[28] and a folded central $Ru_2(N)(H)$ ring (the dihedral angle between two N–Ru–H planes is 40.5°). **A** is 0.9 kcal mol^{-1} less stable than **2a** and easily binds a benzene molecule with an activation free energy of 5.9 kcal mol^{-1} to give the η^2-C_6H_6 adduct **B** and then the μ-η^2:η^2-C_6H_6 adduct **3a″**. The benzene binding reaction **A** + C_6H_6 → **3a″** is exergonic (ΔG = −2.8 kcal mol^{-1}) and exothermic (ΔH = −19.5 kcal mol^{-1}). The small free energy barrier and free energy change for **A** + C_6H_6 → **3a″** are consistent with the facile reversible arene dissociation from **3a** observed experimentally. The endothermicity of C_6H_6 loss from **3a″** indicates that this process is driven by entropy gain.

Next, we compared the behavior of **2a**–**c**. Optimized structures were calculated at B3PW91 level for **2a**–**c**, the corresponding amido hydride complexes **A**, and the transition states (**TS1** and **TS1′**) between **2a**–**c** and **A**. The relative free energies of these species are listed in Table 2. The structures

Table 2. Gibbs Free Energies for the N–H Reductive Elimination from [(Cp*Ru)$_2$(μ-NAr)(μ-H)$_2$] (2a–c) to [(Cp*Ru)$_2$(μ-NHAr)(μ-H)] (A) in C_6H_6 (B3PW91)[a]

Ar	TS1	TS1′	A
Ph	23.8	24.7	8.3
p-$MeOC_6H_4$	24.0	25.9[b]	8.4
p-ClC_6H_4	23.6	24.5	9.2

[a]Energies (kcal mol^{-1}) are relative to **2a**–**c** for each NAr series, Calculated for PCM-optimized structures. [b]Calculated for gas-phase optimized structure with single-point PCM correction.

dx.doi.org/10.1021/ja3005682 | J. Am. Chem. Soc. 2012, 134, 17027–17035

of **2b–c**, **TS1**, **TS1′**, and **A** are similar to the corresponding species in the NPh series. The computed activation energies for the N–H reductive elimination in **2b** are in good agreement with the experimentally observed activation energy for **2b** (22 kcal mol^{-1}). Also, the similarity of computed activation energies for the N–H reductive elimination in **2b** and **2c** is consistent with the similar reaction kinetics for **2b** and **2c**. We also computed kinetic isotope effect for **2b**/**2b**-d_2 and **2c**/**2c**-d_2 by using the approximation $k_H/k_D = \exp\{(\Delta G^{\ddagger}_D - \Delta G^{\ddagger}_H)/RT\}$.[29] For the reaction pathway via **TS1**, we obtained k_H/k_D = 1.59 for **2b**/**2b**-d_2 and k_H/k_D = 1.64 for **2c**/**2c**-d_2. These values are comparable to the experimentally determined KIEs. For the reaction pathway via **TS1′**, smaller KIEs (1.27 for **2b**/**2b**-d_2 and 1.29 for **2c**/**2c**-d_2) were calculated. This may indicate that the pathway via **TS1** might predominate in the real reaction system.

Finally, we computationally examined the reactivity of **2d**. We calculated optimized structures of **2d**, **TS1**, **A** (Ar = 2,6-$Me_2C_6H_3$), and **3d″**; relative Gibbs free energies of these species are shown in Figure 6. The optimized structure of **2d** is

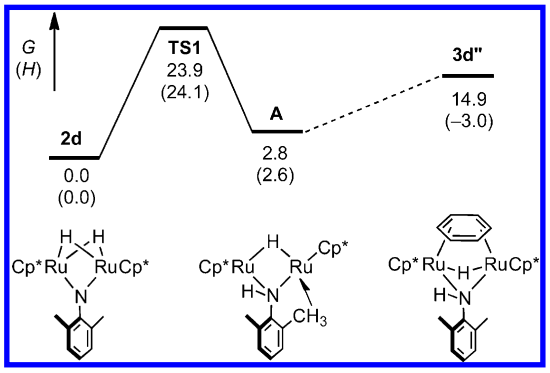

Figure 6. Gibbs free energy profile for **2d** + C_6H_6 → **3d″** in C_6H_6 (M06, PCM). Energies (kcal mol^{-1}) are relative to **2d** + C_6H_6. Enthalpies are given in parentheses.

similar to those of **2a–c**. The optimized structure of **A** (Ar = 2,6-$Me_2C_6H_3$; Figure 4) contains a C–H agostic interaction between a methyl group in the NHAr ligand and one of the Ru centers (CH···Ru = 2.16 Å). Between **2d** and **A**, we found a transition state (**TS1**) that was analogous to the **TS1**s in the other NAr series. The activation energy for the conversion of **2d** to **A** is 23.9 kcal mol^{-1}, which is comparable to that for the conversion of **2a** to **A**. Attempted optimization of **TS1′** for this Ar = 2,6-$Me_2C_6H_3$ system led to convergence to **TS1**. On the other hand, benzene binding to **A** derived from **2d** is energetically highly unfavorable; the free energy of the benzene adduct **3d″** is calculated to be 14.9 kcal mol^{-1} relative to **2d** + C_6H_6. Thus, the apparent lack of reactivity of **2d** under thermal conditions (i.e., toluene, 110 °C) can be ascribed to the instability of the amido hydride arene adduct, which would be too sterically hindered. This view is consistent with the smooth reaction of **2d** with a smaller ligand, CO, at room temperature, which gives the bis-CO adduct of **A** (i.e., complex **6**; eq 5).

The reaction pathways deduced for the N–H reductive elimination in **2a–d** have considerable similarity with those proposed for the NH + H addition reaction on Ru surface (Figure 7).[2] It has been shown that both NH and H occupy the 3-fold hollow sites in their most stable states (Figure 7(a)). In the transition states the NH group is proposed to move toward a bridge site, and the H atom approaches to this group either from a bridge site (Figure 7(b)) or from a top site (Figure 7(b′))

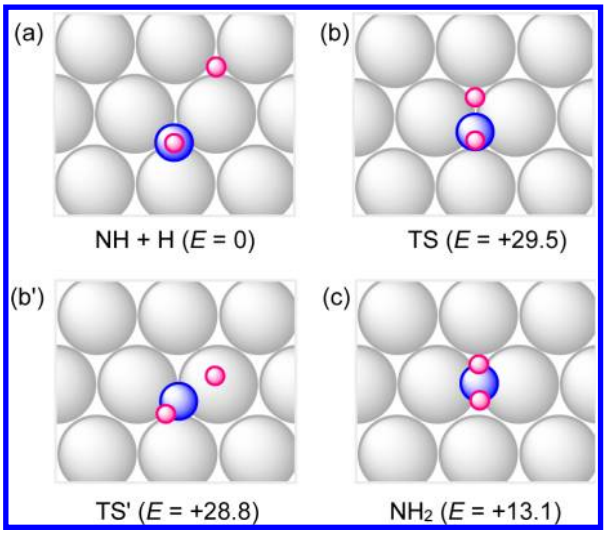

Figure 7. Proposed mechanism of NH + H → NH_2 on Ru(0001) surface.[2a] Relative energies are given in kcal mol^{-1}.

with similar activation energies. The product is an edge-bridging NH_2 (Figure 7(c)), which is less stable than NH + H. Our diruthenium imido dihydride system seems to provide a model for these transition states and reproduce the relative instability of NH_2 species compared to the NH + H pair.

■ CONCLUSIONS

Oxidative addition of H_2 to the bis(amido) complexes **1a–d** induced elimination of $ArNH_2$ via α-H-abstraction to yield the imido dihydride complexes **2a–d**. Complexes **2a–c** underwent the reductive elimination of an N–H bond in the presence of excess arene to give the amido hydride arene complexes **3a–c** and **3a′–c′**. The rate and deuterium kinetic isotope effect were determined for the formation of **3b′,c′**, and it has been proposed that the reaction proceeds with the rate-determining N–H reductive elimination from **2a–c** followed by trapping of the unsaturated amido hydride species [(Cp*Ru)$_2$(μ-NHAr)(μ-H)] (**A**) by an arene molecule. The dimer of **A** (complex **4**), which contains an unprecedented μ_4-NHPh bridge, was isolated and shown to interconvert reversibly with **3a**.

The transition states and energetics for the N–H reductive elimination in **2a–d** was studied by DFT calculations. The calculations indicated that the N–H reductive elimination in **2a–c** can proceed either by maintaining the bridging hydride structure or via the formation of a terminal hydride ligand. This microscopic picture is very similar to that proposed for the NH + H addition reaction on Ru surface.

This work represents the first mechanistic study of imido–hydride reductive elimination in a well-defined organometallic system.

■ EXPERIMENTAL SECTION

General Remarks. All manipulations were performed under an atmosphere of nitrogen using standard Schlenk techniques unless otherwise noted. Aniline and 2,6-dimethylaniline were degassed and stored over activated 4-Å molecular sieves in the dark. Anhydrous solvents (THF, hexane, toluene, diethyl ether, and acetonitrile) were purchased from commercial vendors and degassed before use. Benzene-d_6, cyclohexane-d_{12}, and THF-d_8 were degassed by freeze–pump–thaw cycles and stored over activated 4-Å molecular sieves. [Cp*Ru(μ_3-Cl)]$_4$ and [Cp*Ru(μ-NHPh)]$_2$ (**1a**) were prepared according to the literature.[30,17c] Lithium amides LiNHAr were prepared in situ by deprotonation of $ArNH_2$ with *n*-BuLi in THF at −80 °C. Other reagents were purchased from commercial vendors and used without further purification unless otherwise noted.

dx.doi.org/10.1021/ja3005682 | J. Am. Chem. Soc. 2012, 134, 17027–17035

[Cp*Ru(μ-NHC$_6$H$_4$OMe-*p*)]$_2$ (1b). A solution of LiNHC$_6$H$_4$OMe-*p* (2.66 mmol) in 5 mL of THF was transferred via a cannula to a slurry of [Cp*Ru(μ_3-Cl)]$_4$ (721 mg, 0.663 mmol) in 10 mL of THF at −80 °C. The mixture was allowed to warm to room temperature over 3 h with stirring to give a dark blue solution. The solution was evaporated to dryness, and the residue was extracted with toluene. Recrystallization from toluene−hexane afforded **1b** as dark blue crystals. Yield 488 mg (0.680 mmol, 51%). Anal. Calcd for $C_{34}H_{46}N_2O_2Ru_2$: C, 56.96; H, 6.47; N, 3.91. Found: C, 56.59; H, 6.56; N, 3.62. ^{1}H NMR (400 MHz, C_6D_6): δ 7.50 (m, 4H, aryl), 7.04 (m, 4H, aryl), 3.56 (s, 6H, OMe), 1.43 (s, 30H, Cp*), −1.09 (br, 2H, NH). ^{13}C{^{1}H} NMR (100 MHz, C_6D_6): δ 156.0, 154.5, 122.2, 113.4 (aryl), 73.3 (C_5Me$_5$), 55.3 (OMe), 11.6 (C_5Me_5). IR (Nujol, cm^{-1}): 3213 (w, ν_{NH}).

[Cp*Ru(μ-NHC$_6$H$_4$Cl-*p*)]$_2$ (1c). A solution of LiNHC$_6$H$_4$Cl (3.70 mmol) in 6 mL of THF was transferred via a cannula to a slurry of [Cp*Ru(μ_3-Cl)]$_4$ (1.00 g, 0.922 mmol) in 8 mL of THF at −80 °C. The mixture was allowed to warm to room temperature over 3 h with stirring to give a dark blue solution. The solution was evaporated to dryness, and the residue was extracted with toluene. Recrystallization from toluene−hexane afforded **1c** as a dark blue crystalline solid. Yield 966 mg (1.33 mmol, 72%). Anal. Calcd for $C_{32}H_{40}N_2Cl_2Ru_2$: C, 52.96; H, 5.56; N, 3.86. Found: C, 52.60; H, 5.38; N, 3.73. ^{1}H NMR (400 MHz, C_6D_6): δ 7.33 (d, *J* = 7.9 Hz, 4H, aryl), 7.28 (br, 4H, aryl), 1.26 (s, 30H, Cp*), −1.29 (br, 2H, NH). ^{13}C{^{1}H} NMR (100 MHz, C_6D_6): δ 161.4, 127.9, 124.7, 122.9 (aryl), 73.1 (C_5Me$_5$), 11.3 (C_5Me_5).

[Cp*Ru(μ-NHXy)]$_2$ (1d). A solution of LiNHXy (4.0 mmol) in 6 mL of THF was transferred via a cannula to a slurry of [Cp*Ru(μ_3-Cl)]$_4$ (1.054 g, 0.974 mmol) in 14 mL of THF at −80 °C. The mixture was warmed to 0 °C over 2 h with stirring to give a dark violet solution. The solution was evaporated to dryness, and the residue was extracted with toluene chilled at −10 °C. Recrystallization from toluene−hexane at −30 °C afforded **1d** as a violet crystalline solid. Yield 997 mg (1.40 mmol, 72%). Anal. Calcd for $C_{36}H_{50}N_2Ru_2$: C, 60.65; H, 7.07; N, 3.93. Found: C, 60.20; H, 7.07; N, 3.87. ^{1}H NMR (500 MHz, C_6D_6): δ 7.39 (d, *J* = 7.4 Hz, 2H, aryl), 7.27 (d, *J* = 7.4 Hz, 2H, aryl), 7.01 (t, *J* = 7.4 Hz, 2H, Ar), 3.00 (s, 6H, C$_6$H$_3$*Me*$_2$), 2.32 (s, 6H, C$_6$H$_3$*Me*$_2$), 1.08 (s, 30H, Cp*), −0.14 (br, 2H, NH).

[(Cp*Ru)$_2$(μ-NPh)(μ-H)$_2$] (2a). In a Schlenk flask of ca. 50 mL inner volume, **1a** (232 mg, 0.353 mmol) and 1,3,5-trimethoxybenzene (59.3 mg, 0.353 mmol, internal standard) were dissolved in 15 mL of toluene. After cooling to −80 °C, the flask was evacuated, filled with H_2 (1 atm), and sealed. The mixture was allowed to warm to room temperature over 2 h with stirring to give a dark red solution. ^{1}H NMR analysis showed that **2a** and **3a** were formed in 71% and 26% yield, respectively. ^{1}H NMR for **2a** (500 MHz, C_6D_6): δ 7.55 (d, *J* = 7.4 Hz, 2H, Ph), 7.34 (t, *J* = 7.4 Hz, 2H, Ph), 7.26 (t, *J* = 7.4 Hz, 1H, Ph), 1.83 (s, 30H, Cp*), −11.25 (s, 2H, μ-H, T_1 min = 468 ms (−80 °C, 500 MHz)). ^{13}C{^{1}H} NMR for **2a** (100 MHz, cyclohexane-d_{12}): δ 164.1, 128.3, 122.9, 116.9 (Ph), 92.0 (C_5Me$_5$), 12.2 (C_5Me_5). IR (Nujol, cm^{-1}): 1643 (ν_{RuH}, assigned by comparison with D-isotopomer).

[(Cp*Ru)$_2$(μ-NPh)(μ-D)$_2$] (2a-d_2). In a Schlenk flask of ca. 20 mL inner volume, **1a** (19.5 mg, 0.0297 mmol) and 1,3,5-trimethoxybenzene (5.5 mg, 0.0327 mmol, internal standard) were dissolved in 0.5 mL of toluene-d_8. After cooling to −80 °C, the flask was evacuated, filled with D_2 (1 atm), and sealed. The mixture was allowed to warm to room temperature over 3 h with stirring to give a dark red solution. ^{1}H NMR analysis showed that **2a**-d_2 and PhNH$_2$ were formed in 87% and 100% yield, respectively. Similar experiment in nondeuterated toluene also gave **2a**-d_2 as confirmed by ^{1}H NMR spectroscopy.

[(Cp*Ru)$_2$(μ-NC$_6$H$_4$OMe-*p*)(μ-H)$_2$] (2b). In a Schlenk flask of ca. 50 mL inner volume, **1b** (347 mg, 0.484 mmol) was suspended in 20 mL of hexane. After cooling to −80 °C, the flask was evacuated, filled with H_2 (1 atm), and sealed. The mixture was allowed to warm to room temperature over 3 h with stirring to give a dark red solution. The solution was evaporated under reduced pressure, and the residue was washed with acetonitrile to give **2b** as a red crystalline solid. Yield 177 mg (0.296 mmol, 61%). Anal. Calcd for $C_{27}H_{39}NORu_2$: C, 54.43; H, 6.60; N, 2.35. Found: C, 54.23; H, 6.69; N, 2.34. ^{1}H NMR (400 MHz, C_6D_6): δ 7.72 (d, *J* = 8.8 Hz, 2H, aryl), 6.95 (d, *J* = 8.8 Hz, 2H, aryl), 3.45 (s, 3H, OMe), 1.88 (s, 30H, Cp*), −11.40 (s, 2H, μ-H, T_1 min = 474 ms (−60 °C, 500 MHz)). ^{13}C{^{1}H} NMR (100 MHz, C_6D_6): δ 165.0, 157.3, 120.0, 114.1 (aryl), 91.8 (C_5Me$_5$), 55.1 (OMe), 12.3 (C_5Me_5). IR (Nujol, cm^{-1}): 1650 (ν_{RuH}).

[(Cp*Ru)$_2$(μ-NC$_6$H$_4$Cl-*p*)(μ-H)$_2$] (2c). In a Schlenk flask of ca. 50 mL inner volume, **1c** (417 mg, 0.574 mmol) was dissolved in 20 mL of toluene. After cooling to −80 °C, the flask was evacuated, filled with H_2 (1 atm), and sealed. The mixture was allowed to warm to room temperature over 3 h with stirring to give a dark red solution. The solution was evaporated under reduced pressure, and the residue was recrystallized from THF−MeCN at −30 °C to give **2c** as a red block crystals. Yield 228 mg (0.379 mmol, 67%). Anal. Calcd for $C_{26}H_{36}NClRu_2$: C, 52.03; H, 6.05; N, 2.33. Found: C, 51.55; H, 5.87; N, 2.38. ^{1}H NMR (400 MHz, C_6D_6): δ 7.34 (d, *J* = 8.6 Hz, 2H, aryl), 7.25 (d, *J* = 8.6 Hz, 2H, aryl), 1.79 (s, 30H, Cp*), −11.28 (s, 2H, μ-H, T_1 min = 467 ms (−60 °C, 500 MHz)). ^{13}C{^{1}H} NMR (100 MHz, C_6D_6): δ 170.1, 128.7, 128.1, 118.7 (aryl), 92.0 (C_5Me$_5$), 12.1 (C_5Me_5). IR (Nujol, cm^{-1}): 1590 (ν_{RuH}).

[(Cp*Ru)$_2$(μ-NXy)(μ-H)$_2$] (2d). In a Schlenk flask of ca. 100 mL inner volume, **1d** (729 mg, 1.02 mmol) was dissolved in 42 mL of toluene. After cooling to −80 °C, the flask was evacuated, filled with H_2 (1 atm), and sealed. The solution was allowed to warm to room temperature over 3 h with stirring to give a reddish brown solution. The solution was concentrated under reduced pressure and layered with acetonitrile to gave **2d** as a red crystalline solid. Yield 448 mg (0.755 mmol, 74%). Anal. Calcd for $C_{28}H_{41}NRu_2$: C, 56.64; H, 6.96; N, 2.36. Found: C, 56.62; H, 7.14; N, 2.32. ^{1}H NMR (400 MHz, C_6D_6): δ 7.23 (d, *J* = 7.4 Hz, 2H, aryl), 7.07 (t, *J* = 7.4 Hz, 1H, aryl), 1.83 (s, 6H, C$_6$H$_3$*Me*$_2$), 1.74 (s, 30H, Cp*), −10.98 (s, 2H, μ-H, T_1 min = 476 ms (−80 °C, 500 MHz)). ^{13}C{^{1}H} NMR (100 MHz, C_6D_6): δ 170.8, 127.2, 121.6, 119.9 (aryl), 91.9 (C_5Me$_5$), 18.5 (C$_6$H$_3$*Me*$_2$), 11.7 (C_5Me_5).

[(Cp*Ru)$_2$(μ-NHPh)(μ-H)(μ-η^2:η^2-C$_7$H$_8$)] (3a). In a Schlenk flask of ca. 100 mL inner volume, **1a** (1.80 g, 2.74 mmol) was dissolved in 45 mL of toluene. After cooling to −80 °C, the flask was evacuated, filled with H_2 (1 atm), and sealed. The mixture was allowed to warm to room temperature over 2 h with stirring to yield a dark red solution. The H_2 gas was removed by evacuation, and the solution was stirred under N_2 for additional 12 h at room temperature. The solution was concentrated under reduced pressure and layered with acetonitrile. After diffusion of the solvents was complete, **3a** was isolated as a red solid. Yield 1.23 g (1.87 mmol, 68%). Anal. Calcd for $C_{33}H_{45}NRu_2$: C, 60.25; H, 6.89; N, 2.13. Found: C, 60.07; H, 7.08; N, 2.09. ^{1}H NMR (500 MHz, C_6D_6): δ 6.98 (br, 2H, Ph), 6.71 (t, *J* = 7.4 Hz, 1H, Ph), 6.65 (br, 2H, Ph), 1.50 (s, 30H, Cp*), −1.38 (br, 1H, NH), −13.72 (s, 1H, μ-H). ^{13}C{^{1}H} NMR (100 MHz, C_6D_6, 80 °C): δ 164.1, 127.8, 123.1, 119.3 (Ph), 89.9 (C_5Me$_5$), 9.9 (C_5Me_5). IR (Nujol, cm^{-1}): 3210 (w, ν_{NH}), 1597 (w, ν_{RuH}); the assignment was confirmed by red shift in **3a**-d_2: ν_{ND} = 2387 cm^{-1}, ν_{RuD} obscured by other peaks. ^{1}H NMR (500 MHz, THF-d_8, −80 °C, in the presence of 10 equiv of toluene): δ 7.00 (t, 1H, *J* = 7.6 Hz, NHP*h*), 6.73 (t, 1H, *J* = 7.6 Hz, NHP*h*), 6.56 (t, 1H, *J* = 7.6 Hz, NHP*h*), 6.46 (d, 1H, *J* = 7.6 Hz, NHP*h*), 6.32 (t, 1H, *J* = 7.6 Hz, NHP*h*), 5.67 (d, 1H, *J* = 5.5 Hz, C$_6$*H*$_5$Me), 3.03 (d, 1H, *J* = 5.5 Hz, C$_6$*H*$_5$Me), 2.91 (d, 1H, *J* = 6.7 Hz, C$_6$*H*$_5$Me), 2.86−2.79 (m, 2H, C$_6$*H*$_5$Me), 1.93 (s, 3H, C$_6$H$_5$*Me*), 1.56 (s, 15H, Cp*), 1.50 (s, 15H, Cp*), −1.83 (br, 1H, NH), −13.85 (s, 1H, μ-H). ^{13}C{^{1}H} NMR (100 MHz, THF-d_8, −80 °C, in the presence of 10 equiv of toluene): δ 164.0, 130.9 (C$_6$H$_4$Me), 127.6, 127.5, 125.2, 120.1 (NHPh), 119.2 (C$_6$H$_4$Me), 116.6 (NHPh), 89.6, 89.0 (C_5Me$_5$), 56.7, 53.9, 51.2, 50.4 (C$_6$H$_4$Me), 21.3 (C$_6$H$_4$*Me*), 10.1, 9.9 (C_5Me_5).

[(Cp*Ru)$_2$(μ-NHC$_6$H$_4$OMe-*p*)(μ-H)(μ-η^2:η^2-C$_7$H$_8$)] (3b). **2b** (63 mg, 0.106 mmol) was dissolved in 5 mL of toluene, and the solution was stirred at 35 °C for 24 h. Removal of the solvent in vacuo yielded **3b** as a red solid. Yield 72 mg (0.104 mmol, 98%). ^{1}H NMR (400 MHz, C_6D_6): δ 6.61 (m, 4H, aryl), 3.37 (s, 3H, OMe), 1.52 (s, 30H, Cp*), −1.36 (br, 1H, NH), −13.81 (s, 1H, μ-H). ^{13}C{^{1}H} NMR (100 MHz, C_6D_6): δ 157.3, 153.4, 121.2, 113.0 (aryl), 89.8 (C_5Me$_5$), 55.1 (OMe), 10.1 (C_5Me_5). IR (Nujol, cm^{-1}): 3211 (w, ν_{NH}), 1607 (w, ν_{RuH}); the assignment was confirmed by red shift in **3b**-d_2: ν_{ND} = 2386 cm^{-1}, ν_{RuD} obscured by other peaks.

dx.doi.org/10.1021/ja3005682 | J. Am. Chem. Soc. 2012, 134, 17027−17035

[(Cp*Ru)$_2$(μ-NHC$_6$H$_4$Cl-*p*)(μ-H)(μ-η^2:η^2-C$_7$H$_8$)] (3c). **2c** (43.2 mg, 0.072 mmol) was dissolved in 5 mL of toluene, and the solution was stirred at 35 °C for 24 h. Removal of the solvent in vacuo yielded **3c** as a red solid. Yield 49.3 mg (0.071 mmol, 99%). ^{1}H NMR (400 MHz, C_6D_6): δ 6.92 (br, 2H, aryl), 6.92 (d, J = 6.4 Hz, 2H, aryl), 1.43 (s, 30H, Cp*), −1.65 (br, 1H, NH), −13.72 (s, 1H, μ-H). ^{13}C{^{1}H} NMR (100 MHz, C_6D_6): δ 163.1, 128.2, 127.9, 123.2 (aryl), 89.6 (C_5Me$_5$), 10.0 (C_5*Me*$_5$). IR (Nujol, cm^{-1}): 3207 (w, ν_{NH}), 1594 (w, ν_{RuH}); the assignment was confirmed by red shift in **3c**-d_2: ν_{ND} = 2385 cm^{-1}, ν_{RuD} obscured by other peaks.

[(Cp*Ru)$_4$(μ_4-NHPh)(μ-NHPh)(μ-H)$_2$] (4). **3a** (130 mg, 0.198 mmol) was dissolved in THF (1 mL), and the solution was stirred for 5 min. Layering 3 mL of acetonitrile onto this solution gave dark brown block crystals of **4**. The crystals were used for the single-crystal X-ray study. Yield 88 mg (0.0778 mmol, 79%). Anal. Calcd for $C_{52}H_{74}N_2Ru_4$: C, 55.20; H, 6.59; N, 2.48. Found: C, 55.27; H, 6.60; N, 2.54. ^{1}H NMR (400 MHz, THF-d_8): δ 6.83 (br, 2H, Ph), 6.50 (m, 3H, Ph), 5.10 (br, 1H, NH), 2.73 (m, 3H, μ_4-NH*Ph*), 2.50 (d, J = 7.2 Hz, 1H, μ_4-NH*Ph*), 1.96 (m, 1H, μ_4-NH*Ph*), 1.78, 1.67, 1.56, 1.46 (s, 15 H each, Cp*), 0.66 (brs, 1H, NH), −9.49 (s, 1H, μ-H), −13.63 (s, 1H, μ-H). ^{13}C{^{1}H} NMR (100 MHz, THF-d_8, 60 °C): δ 165.4, 128.8, 124.2, 120.2 (Ph), 92.0, 90.6, 85.4, 74.1 (C_5Me$_5$), 114.8, 57.7, 54.3, 49.7, 48.5, 34.1 (μ_4-NH*Ph*), 13.9, 12.9, 11.2, 11.1 (C_5*Me*$_5$). IR (Nujol, cm^{-1}): 3277, 3170 (w, ν_{NH}).

[(Cp*Ru)$_2$(μ-NHPh)(μ-H)(μ-η^2:η^2-C$_{10}$H$_8$)] (5a). To a solution of **3a** (59 mg, 0.090 mmol) in 4 mL of THF was added naphthalene (14 mg, 0.107 mmol), and the solution was stirred for 1 h at room temperature. Recrystallization from THF−MeCN gave **5a** as red plate crystals. Yield 92.6 mg (0.134 mmol, 100%). Anal. Calcd for $C_{36}H_{45}NRu_2$: C, 62.31; H, 6.54; N, 2.02. Found: C, 62.69; H, 6.67; N, 2.06. ^{1}H NMR (400 MHz, C_6D_6): δ 7.44, 7.19 (dd, J = 5.3, 3.2 Hz, 2H each, $C_{10}H_8$), 6.94 (br, 1H, Ph), 6.60 (m, 3H, Ph), 5.64 (br, 1H, Ph), 3.71, 3.05 (dd, J = 5.3, 3.2 Hz, 2H each, μ-η^2:η^2-$C_{10}H_8$), 1.50 (s, 30H, Cp*), −1.26 (br, 1H, NH), −13.44 (s, 1H, μ-H). ^{13}C{^{1}H} NMR (100 MHz, C_6D_6, 80 °C): δ 163.0, 136.9, 127.7, 125.3, 124.7, 122.4, 119.1 (aryl), 90.5 (C_5Me$_5$), 52.5, 49.6 (μ-η^2:η^2-$C_{10}H_8$), 10.0 (C_5*Me*$_5$). IR (Nujol, cm^{-1}): 3265 (w, ν_{NH}), 1652 (w, ν_{RuH}).

[(Cp*Ru)$_2$(μ-NHXy)(μ-H)(CO)$_2$] (6). A solution of **2d** (130 mg, 0.213 mmol) in 10 mL of toluene was stirred under 1 atm of CO at room temperature for 2 h. The resulting red solution was evaporated to dryness, and the residue was recrystallized from hexane at −30 °C to give **6** as red crystalline solid. Yield 101 mg (0.155 mmol, 73%). Anal. Calcd for $C_{30}H_{41}NO_2Ru_2$: C, 55.45; H, 6.36; N, 2.16. Found: C, 55.42; H, 6.78; N, 2.07. ^{1}H NMR (400 MHz, C_6D_6): δ 7.00 (t, J = 7.2 Hz, 2H, aryl), 6.85 (t, J = 7.2 Hz, 1H, aryl), 4.31 (br, 1H, NH), 2.77, 2.52 (s, 3H each, C_6H_3*Me*$_2$), 1.71, 1.55 (s, 15H each, Cp*), −13.99 (s, 1H, μ-H). ^{13}C{^{1}H} NMR (100 MHz, C_6D_6): δ 206.5, 206.2 (CO), 152.6, 131.6, 131.3, 129.3, 128.8, 121.1 (aryl), 94.4, 94.3 (C_5Me$_5$), 23.0, 21.3 (C_6H_3*Me*$_2$), 10.4, 10.0 (C_5*Me*$_5$). IR (Nujol, cm^{-1}): 3330 (w, ν_{NH}), 2009, 1891 (s, ν_{CO}), 1619 (w, ν_{RuH}).

Kinetic Experiments. The following operation is representative. **2b** (19.4 mg, 0.0326 mmol) and 1,3,5-trimethoxybenzene (5.1 mg) as internal standard were dissolved in a mixture of cyclohexane-d_{12} (0.50 mL) and benzene-d_6 (144 μL, 1.63 mmol), and the solution was transferred to an NMR tube by a syringe. After being flame-sealed, the tube was loaded onto an NMR probe and kept at constant temperature. ^{1}H NMR spectra were taken at every 10 min, and the concentration [**2b**] was determined by integrating the Cp* resonance of **2b** relative to the internal standard. The rate constant k_{obs} was obtained by a linear plot of ln([**2b**]/[**2b**]$_0$) against time (s).

X-ray Crystallography. Single crystals of **4** and **5a** were obtained as described in the synthetic procedure section. All measurements were performed on a Rigaku R-AXIS Rapid imaging plate detector with graphite monochromated Mo Kα radiation (λ = 0.71069 Å). The frame data were processed using the PROCESS-AUTO program,[31] and the reflection data were corrected for absorption with ABSCOR program.[32] The structures were solved by SHELXS-97 and refined by SHELXL-97.[33] Non-hydrogen atoms were refined with anisotropic displacement parameters. The metal-bound hydrogen atoms in **4** and **5a** and the N−H hydrogen atoms in **4** could not be located by the difference Fourier method and were not included in the structure. Other hydrogen atoms were placed at calculated positions and treated as riding models. Thermal ellipsoid plots were drawn by ORTEP-3 for Windows.[34] Detailed crystallographic data are given in the Supporting Information.

Computational Details. All calculations were performed with Gaussian 09 program[35] using the M06[36] or B3PW91[37] functionals with LanL2DZ effective core pseudopotential and basis set[38] for Ru and 6-31G(d,p) basis set[39] for all other atoms. Geometry optimizations were performed without any symmetry constraints and in the presence of C_6H_6 solvent using the polarizable continuum model[40] unless otherwise mentioned. Local minima and transition states were checked by analytical frequency calculations, and intrinsic reaction coordinate calculations and subsequent geometry optimizations were used to confirm the connection of each transition state with corresponding local minima. Gibbs free energies are those in C_6H_6 solution and at 298.15 K and 1 atm.

■ ASSOCIATED CONTENT

Ⓢ Supporting Information

Crystallographic data in CIF format; coordinates and energies of calculated complexes; and complete ref 35. This material is free of charge via the Internet at http://pubs.acs.org.

■ AUTHOR INFORMATION

Corresponding Author

matuzaka@c.s.osakafu-u.ac.jp

Notes

The authors declare no competing financial interest.

■ ACKNOWLEDGMENTS

This work was supported by a Grant-in-Aid for Scientific Research (C) and a Grant-in-Aid for Scientific Research on Innovative Areas "Molecular Activation Directed toward Straightforward Synthesis" from the Ministry of Education, Science, Sports, and Culture of Japan. We also thank financial support from Toyota Motor Corporation.

■ REFERENCES

(1) Ertl, G. In *Catalytic Ammonia Synthesis*; Jennings, J. R., Ed.; Plenum Press: New York, 1991; pp 109−131.

(2) (a) Zhang, C. J.; Lynch, M.; Hu, P. *Surf. Sci.* **2002**, *496*, 221. (b) Honkala, K.; Hellman, A.; Remediakis, I. N.; Logadottir, A.; Carlsson, A.; Dahl, S.; Christensen, C. H.; Nørskov, J. K. *Science* **2005**, *307*, 555. (c) McKay, H. L.; Jenkins, S. J.; Wales, D. J. *J. Phys. Chem. C* **2009**, *113*, 15274. (d) Macgregor, S. A. *Organometallics* **2001**, *20*, 1860.

(3) (a) Cowan, R. L.; Trogler, W. C. *J. Am. Chem. Soc.* **1989**, *111*, 4750. (b) Glueck, D. S.; Newman Winslow, L. J.; Bergman, R. G. *Organometallics* **1991**, *10*, 1462. (c) Zhao, J.; Goldman, A. S.; Hartwig, J. F. *Science* **2005**, *307*, 1080. (d) Sykes, A. C.; White, P.; Brookhart, M. *Organometallics* **2006**, *25*, 1664.

(4) (a) Eikey, R. A.; Abu-Omar, M. M. *Coord. Chem. Rev.* **2003**, *243*, 83. (b) Li, Y.; Wong, W.-T. *Coord. Chem. Rev.* **2003**, *243*, 191.

(5) (a) Cummins, C. C.; Baxter, S. M.; Wolczanski, P. T. *J. Am. Chem. Soc.* **1988**, *110*, 8731. (b) Dobbs, D. A.; Bergman, R. G. *J. Am. Chem. Soc.* **1993**, *115*, 3836. (c) Blake, R. E.; Antonelli, D. M.; Henling, L. M.; Schaefer, W. P.; Hardcastle, K. I.; Bercaw, J. E. *Organometallics* **1998**, *17*, 718. (d) Brown, S. D.; Peters, J. C. *J. Am. Chem. Soc.* **2004**, *126*, 4538. (e) Hanna, T. E.; Keresztes, I.; Lobkovsky, E.; Bernskoetter, W. H.; Chirik, P. J. *Organometallics* **2004**, *23*, 3448. (f) Bart, S. C.; Lobkovsky, E.; Bill, E.; Chirik, P. J. *J. Am. Chem. Soc.* **2006**, *128*, 5302. (g) Ishiwata, K.; Kuwata, S.; Ikariya, T. *J. Am. Chem. Soc.* **2009**, *131*, 5001. (h) Kimura, T.; Koiso, N.; Ishiwata, K.; Kuwata, S.; Ikariya, T. *J. Am. Chem. Soc.* **2011**, *133*, 8880.

(6) (a) Brown, S. D.; Mehn, M. P.; Peters, J. C. *J. Am. Chem. Soc.* **2005**, *127*, 13146. (b) Askevold, B.; Nieto, J. T.; Tussupbayev, S.; Diefenbach, M.; Herdtweck, E.; Holthausen, M. C.; Schneider, S. *Nature Chem.* **2011**, *3*, 532. (c) Rodriguez, M. M.; Bill, E.; Brennessel, W. W.; Holland, P. L. *Science* **2011**, *334*, 780.
(7) For an intermolecular nitride−hydride coupling, see: Yi, X.-Y.; Ng, H.-Y.; Williams, I. D.; Leung, W.-H. *Inorg. Chem.* **2011**, *50*, 1161.
(8) (a) Fryzuk, M. D.; Love, J. B.; Rettig, S. J.; Young, V. G. *Science* **1997**, *275*, 1445. (b) Pool, J. A.; Lobkovsky, E.; Chirik, P. J. *Nature* **2003**, *427*, 527. (c) MacLaclan, E. A.; Hess, F. M.; Patrick, B. O.; Fryzuk, M. D. *J. Am. Chem. Soc.* **2007**, *129*, 10895. (d) Pun, D.; Bradley, C. A.; Lobkovsky, E.; Keresztes, I.; Chirik, P. J. *J. Am. Chem. Soc.* **2008**, *130*, 14046.
(9) (a) Yin, C. C.; Deeming, A. J. *J. Chem. Soc., Dalton Trans.* **1974**, 1013. (b) Smieja, J. A.; Stevens, R. E.; Fjare, D. E.; Gladfelter, W. L. *Inorg. Chem.* **1985**, *24*, 3206. (c) Arita, H.; Ishiwata, K.; Kuwata, S.; Ikariya, T. *Organometallics* **2008**, *27*, 493.
(10) Baranger, A. M.; Bergman, R. G. *J. Am. Chem. Soc.* **1994**, *116*, 3822.
(11) Kameo, H.; Nakajima, Y.; Suzuki, H. *Eur. J. Inorg. Chem.* **2007**, 1793.
(12) (a) Ozaki, A. *Acc. Chem. Res.* **1981**, *14*, 16. (b) Aika, K. *Angew. Chem., Int. Ed.* **1986**, *25*, 558.
(13) (a) Nakajima, Y.; Suzuki, H. *Organometallics* **2003**, *22*, 959. (b) Nakajima, Y.; Inagaki, A.; Suzuki, H. *Organometallics* **2004**, *23*, 4040. (c) Nakajima, Y.; Suzuki, H. *Organometallics* **2005**, *24*, 1860. (d) Nakajima, Y.; Kameo, H.; Suzuki, H. *Angew. Chem., Int. Ed.* **2006**, *45*, 950.
(14) (a) Omori, H.; Suzuki, H.; Take, Y.; Moro-oka, Y. *Organometallics* **1989**, *8*, 2270. (b) Tada, K.; Oishi, M.; Suzuki, H.; Tanaka, M. *Organometallics* **1996**, *15*, 2422.
(15) Jahncke, M.; Neels, A.; Stoeckli-Evans, H.; Süss-Fink, G. *J. Organomet. Chem.* **1998**, *565*, 97.
(16) Kimura, T.; Arita, H.; Ishiwata, K.; Kuwata, S.; Ikariya, T. *Dalton Trans.* **2009**, 2912.
(17) (a) Takemoto, S.; Kobayashi, T.; Matsuzaka, H. *J. Am. Chem. Soc.* **2004**, *126*, 10802. (b) Takemoto, S.; Morita, H.; Karitani, K.; Fujiwara, H.; Matsuzaka, H. *J. Am. Chem. Soc.* **2009**, *131*, 18026. (c) Takemoto, S.; Kobayashi, T.; Ito, T.; Inui, A.; Karitani, K.; Katagiri, S.; Masuhara, Y.; Matsuzaka, H. *Organometallics* **2011**, *30*, 2160.
(18) Blake, R. E., Jr.; Heyn, R. H.; Tilley, T. D. *Polyhedron* **1992**, *11*, 709.
(19) There are two conventions for the electron counting of μ-hydride ligands: the half-electron method and the half-arrow method. See for detail: Parkin, G. In *Comprehensive Organometallic Chemistry III*; Crabtree, R. H., Mingos, D. M. P., Eds; Elsevier: Oxford, UK, 2007; Vol. *1*, Ch. 1. Throughout this article we adopt the half-arrow method. By doing so and assuming the NPh ligand as a four-electron donor, **2a** is a 36-electron complex, for which no Ru−Ru bond should be drawn.
(20) Suzuki, H.; Omori, H.; Lee, D. H.; Yoshida, Y.; Fukushima, M.; Tanaka, M.; Moro-oka, Y. *Organometallics* **1994**, *13*, 1129.
(21) Hamilton, D. G.; Crabtree, R. H. *J. Am. Chem. Soc.* **1988**, *110*, 4126.
(22) Hlatky, G. G.; Crabtree, R. H. *Coord. Chem. Rev.* **1985**, *65*, 1.
(23) For example, see: (a) Chan, D. M.-T.; Fultz, W. C.; Nugent, W. A.; Roe, D. C.; Tulip, T. H. *J. Am. Chem. Soc.* **1985**, *107*, 251. (b) Walsh, P. J.; Hollander, F. J.; Bergman, R. G. *J. Am. Chem. Soc.* **1988**, *110*, 8729. (c) Glueck, D. S.; Wu, J.; Hollander, F. J.; Bergman, R. G. *J. Am. Chem. Soc.* **1991**, *113*, 2041. (d) Zambrano, C. H.; Profilet, R. D.; Hill, J. E.; Fanwick, P. E.; Rothwell, I. P. *Polyhedron* **1993**, *12*, 689. (e) Takemoto, S.; Otsuki, S.; Kamikawa, K.; Matsuzaka, H. *J. Am. Chem. Soc.* **2008**, *130*, 8904. See also ref 17a.
(24) The assignment of ν_{RuH} and ν_{NH} for **3a**−**c** was confirmed by comparison with the IR spectra of deuterium isotopomers **3a**-d_2, **3b**-d_2, and **3c**-d_2. See Experimental Section for details.
(25) Kuhlman, R.; Folting, K.; Caulton, K. G. *Organometallics* **1995**, *14*, 3188.
(26) (a) Nevinger, L. R.; Keister, J. B. *Organometallics* **1990**, *9*, 2312. (b) Tussupbayev, S.; Vyboishchikov, S. F. *Organometallics* **2007**, *26*, 56.
(27) (a) Kee, T. P.; Park, L. Y.; Robbins, J.; Schrock, R. R. *J. Chem. Soc., Chem. Commun.* **1991**, 121. (b) Hankin, D. M.; Danapoulos, A. A.; Wilkinson, G.; Sweet, T. K. N.; Hursthouse, M. B. *J. Chem. Soc., Dalton Trans.* **1996**, 4063. (c) Burrell, A. K.; Steedman, A. *J. Organometallics* **1997**, *16*, 1203.
(28) (a) Ward, T. R.; Schafer, O.; Daul, C.; Hofmann, P. *Organometallics* **1997**, *16*, 3207. (b) Brunner, H.; Tsuno, T. *Acc. Chem. Res.* **2009**, *42*, 1501.
(29) (a) Wiberg, K. B. *Chem. Rev.* **1955**, *55*, 713. (b) Geimer, J.; Beckert, D.; Jenichen, A. *Chem. Phys. Lett.* **1997**, *280*, 353.
(30) Fagan, P. J.; Ward, M. D.; Calabrese, J. C. *J. Am. Chem. Soc.* **1989**, *111*, 1698.
(31) *PROCESS AUTO*, Automatic Data Acquisition and Processing Package for Imaging Plate Diffractometer; Rigaku Corp.: Tokyo, Japan, 1998.
(32) Higashi, T. *ABSCOR*, Empirical Absorption Correction Based on Fourier Series Approximation; Rigaku Corp.: Tokyo, Japan, 1995.
(33) Sheldrick, G. M. *SHELX97*, Program for Crystal Structure Determination; University of Göttingen: Göttingen, Germany, 1997.
(34) ORTEP-3 for Windows: Farrugia, L. J. *J. Appl. Crystallogr.* **1997**, *30*, 565.
(35) Frisch, M. J.; et al. *Gaussian 09*, Revision C.01; Gaussian, Inc.: Wallingford, CT, 2010.
(36) Zhao, Y.; Truhlar, D. G. *Theor. Chem. Acc.* **2008**, *120*, 215.
(37) (a) Becke, A. D. *J. Chem. Phys.* **1993**, *98*, 5648. (b) Perdew, J. P.; Wang, Y. *Phys. Rev.* **1992**, *B45*, 13244.
(38) Wadt, W. R.; Hay, P. J. *J. Chem. Phys.* **1985**, *82*, 284.
(39) Hehre, W. J.; Ditchfield, R.; Pople, J. A. *J. Chem. Phys.* **1972**, *56*, 2257.
(40) Tomasi, J.; Mennucci, B.; Cammi, R. *Chem. Rev.* **2005**, *105*, 2999.